

See discussions, stats, and author profiles for this publication at: <https://www.researchgate.net/publication/231206262>

Laser-Induced Breakdown Spectroscopy for Real-Time Detection of Halon Alternative Agents

ARTICLE *in* ANALYTICAL CHEMISTRY · FEBRUARY 1998

Impact Factor: 5.64 · DOI: 10.1021/ac970362y

CITATIONS

35

READS

8

4 AUTHORS, INCLUDING:



Kevin Mcnesby

Army Research Laboratory

111 PUBLICATIONS 1,352 CITATIONS

SEE PROFILE

Laser-Induced Breakdown Spectroscopy for Real-Time Detection of Halon Alternative Agents

Cynthia K. Williamson,[†] Robert G. Daniel, Kevin L. McNesby, and Andrzej W. Miziolek*

U.S. Army Research Laboratory, AMSRL-WM-BD, Aberdeen Proving Ground, Maryland 21005-5066

We report the results of an evaluation of laser-induced breakdown spectroscopy (LIBS) for the detection of candidate halon replacement compounds (CF_4 , CF_3H , CF_2H_2 , $\text{C}_2\text{F}_5\text{H}$). The fundamental ($1.064\ \mu\text{m}$) from a Nd:YAG Q-switched pulsed laser was focused into an air flow containing 0.0005–5% of the analyte halocarbon compounds. The laser-produced plasma emission consists of a large number of intense fluorine atom lines in the 600–850 nm spectral range. Limit-of-detection studies indicate that LIBS can detect these compounds in the parts per million range. Also, we have recorded single-shot LIBS spectra with good signal-to-noise ratios using an intensified photodiode array. Our results indicate that LIBS is a promising detection technique for in situ and real-time measurement of halons during use in full-scale fire suppression testing.

Halons (halogenated hydrocarbons) are principally used for fire extinguishing applications. Halons 1301 (CF_3Br) and 1211 (CF_2ClBr) are the primary compounds currently used by the military for fire suppression in various weapons systems. The eventual replacement of these compounds is of interest because of the ozone depletion potential (ODP) of bromine- and chlorine-containing compounds.¹ Virtually all of the halons released on the earth's surface eventually reach the stratosphere (ozone layer) through convection from the troposphere.² At high altitudes, the halons are photochemically degraded and the Br and Cl atoms become accessible for reaction with ozone and other atmospheric species.^{1,2} The production of new halons has been prohibited since January 1, 1994, in accordance with the Copenhagen Amendments to the Montreal Protocol on Substances that Deplete the Ozone Layer (Fourth Meeting of the Parties to the Montreal Protocol 1992).

The candidate alternative compounds which are studied in this report are as follows (commercial names): $\text{C}_2\text{F}_5\text{H}$ (FE25, HFC125), CF_4 (FE14), CF_3H (FE13, HFC23), and CF_2H_2 (FE12, HFC32). The detection of the alternative agents is of practical concern in order to monitor their concentrations during full-scale fire sup-

pression testing and to ascertain their effect on atmospheric chemistry. A routine method for real-time and in-situ detection of these compounds has not been previously reported. The development of a routine method has potential applications for field detection where identification, quantitation, and distribution are important parameters. Laser-induced breakdown spectroscopy (LIBS) is investigated here as a method for the detection of halon alternatives. The emission of fluorine, which is liberated in a plasma, is used for the analysis.

LIBS is a well-established technique based on the formation of a laser-induced plasma of the analyte.³ A pulsed laser beam is focused to a fluence of approximately 10^8 to $10^9\ \text{W}/\text{cm}^2$ on or in the sample, which produces an avalanche of ionization or dielectric breakdown of the sample. The laser induces multiphoton ionization which generates an initial electron density.⁴ Continuum absorption of the laser radiation by the free electrons occurs, and electron collisions further ionize and heat the sample. The electron collisions directly generate the plasma by cascade ionization and, thus, breakdown the sample. The emission of the atomic and molecular constituents which are excited within the plasma is then collected with lenses or fiber optics. Typical LIBS plasma temperatures are in the 20 000–25 000 K range for gases at atmospheric pressure.⁴

The instrumentation required for the LIBS experiment is simple compared to other atomic techniques such as ICP and conventional electrode arc and spark spectroscopy. Complicated sample introduction equipment and electrodes are not necessary for the LIBS experiment. Also, LIBS has the capability of being used in situ, while ICP is not readily field deployable.⁵ A standard sample chamber or probe can be implemented in LIBS; wavelength selection is accomplished by a monochromator or acousto-optic tunable filter, and a photomultiplier tube (PMT), photodiode array, or CCD is used for signal detection. Time resolution of the LIBS signal is often performed due to the presence of a strong background plasma continuum emission ($<2\ \mu\text{s}$) immediately following plasma generation. We have found the optimum delay for the detection of atomic analytes is from 1 to $2\ \mu\text{s}$ out to 10–20 μs , depending on the analyte.

The majority of the LIBS studies have involved solid samples (e.g., paper, soils, paint, metals, steel); LIBS analysis of gaseous samples have been reported for the detection of F, Cl, S, P, As,

* To whom correspondence should be sent: (e-mail) miziolek@arl.mil.

[†] NAS/NRC Postdoctoral Research Associate. Present Address: NASA Langley Research Center, Atmospheric Sciences Division, Mail Stop 401A, Hampton, Virginia 23681-0001.

(1) Wuebbles, D. J.; Connell, P. S.; Patten, K. O. *Halon Replacements: Technology and Science*; Miziolek, A. W., Tsang, W., Eds.; ACS Symposium Series 611; American Chemical Society: Washington, DC, 1995; pp 59–71.

(2) Solomon, S.; Garcia, R. R.; Ravishankara, A. R. *J. Geophys. Res.* **1994**, *99*, 20491–20499.

(3) Radziemski, L. J.; Cremers, D. A. *Laser-Induced Plasmas and Applications*; Marcel Dekker: New York, 1989.

(4) Simeonsson, J. B.; Miziolek, A. W. *Appl. Opt.* **1993**, *32*, 939–947.

(5) Yamamoto, K. Y.; Cremers, D. A.; Ferris, M. J.; Foster, L. E. *Appl. Spectrosc.* **1996**, *50*, 222–233.

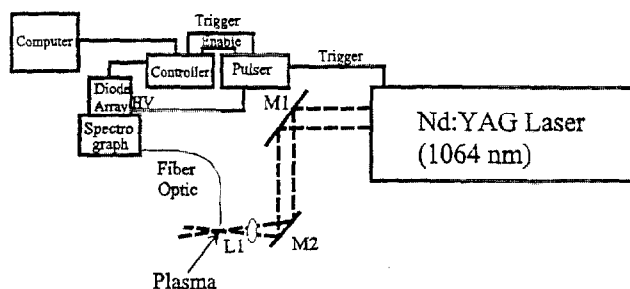


Figure 1. Schematic of photodiode array-based detection system (M = mirror, L = lens, PD = photodiode).

and Hg in air and column III, V hydrides (e.g., B_2H_6 , PH_3).⁶⁻¹¹ The intent of the studies was the measurement of trace amounts of analytes in hostile environments and gas impurities for the hydride work. Hg was detected at the parts per billion level in air using a photodiode array detection system which recorded single-shot spectra over a range of 20 nm.⁸ Cremers et al. reported limits of detection of 8 and 38 ppm for chlorine and fluorine, respectively.¹¹ SF_6 and chlorinated fluorocarbons (e.g., $C_2Cl_3F_3$) were the source compounds. The LIBS signal was time-resolved using a PMT/boxcar averager for detection. A class of halon replacement compounds of particular interest is the hydrofluorocarbons (HFCs). C_2F_5H (FE-25) and CF_3H (FE-13) are candidates for military aircraft and ground combat vehicle engine compartment protection use.

The objective of the present study is the characterization of LIBS for the detection of halon alternatives. The ultimate goal is the application of this technique in a severely hostile fire suppression testing environment. Spectra are recorded neat and in air since this is the most probable environment for samples collected in the field or analyzed in situ. The optimization of parameters unique to our system and an initial description of a practical field device for fire extinguishing applications are described. Some methods for selective detection using LIBS are also considered.

EXPERIMENTAL SECTION

A schematic of the instrumental setup involving the photodiode array-based detection system is shown in Figure 1. The Nd:YAG laser was operated at a repetition rate of 10 Hz and a wavelength of 1064 nm. A photodiode illuminated by the laser radiation was the trigger source for the oscilloscope, boxcar (Stanford Research Systems, SR280), and pulser/photodiode array intensifier (Princeton Instruments PG-10/Princeton Instruments IRY1024G). The emission from the plasma was detected with a photomultiplier tube (EMI-Gencom Inc., 9658R) or gated photodiode array. Optical relay lenses were used to collect the emission for the PMT system, and a single-strand fiber optic (Thorlabs, FP-600-UHT)

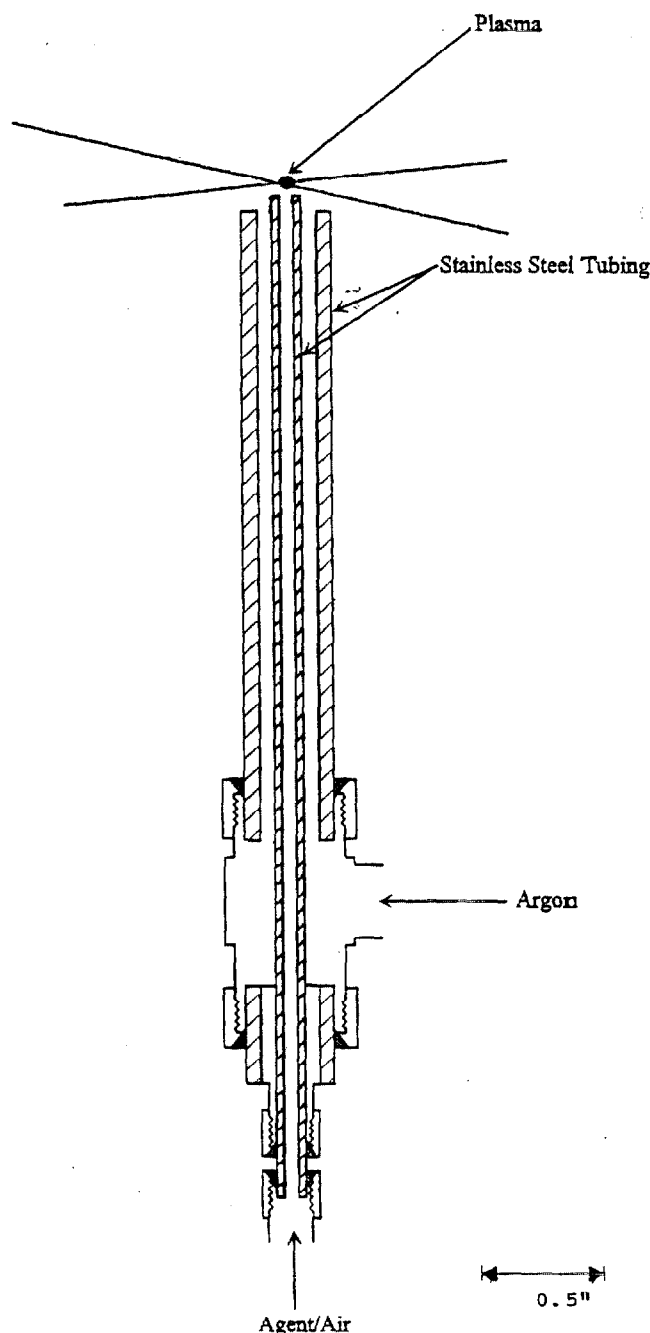


Figure 2. Diagram of the sample-flow apparatus constructed from stainless steel tubing and swagelock connections.

was used in the photodiode array system. Data acquisition was computer-controlled with an SRS (Stanford Research Systems, 465) interface for the PMT system. The laser energy was measured with an energy meter (Scientech Vector, S200). The sample flow apparatus (Figure 2) was constructed from stainless steel tubing and swagelock connections and is similar to the configuration reported by Locke et al.¹² Argon flowed through the outer tube which functioned as a sheath and minimized the mixing of the analyte with room air. The inner tube contained the analyte/air flow. The sample flow apparatus was mounted on a three-dimensional stage in order to adjust the location of

- (6) Cheng, E. A. P.; Fraser, R. D.; Eden, J. G. *Appl. Spectrosc.* **1991**, *45*, 949-952.
- (7) Casini, M.; Harith, M. A.; Palleschi, V.; Salvetti, A.; Singh, D. P.; Vaselli, M. *Laser Part. Beams* **1991**, *9*, 633-639.
- (8) Lazzari, C.; De Rosa, M.; Rastelli, S.; Ciucci, A.; Palleschi, V.; Salvetti, A. *Laser Part. Beams* **1994**, *12*, 525-530.
- (9) Hakkanen, H. J.; Korppi-Tommola, J. E. I. *Appl. Spectrosc.* **1995**, *49*, 1721-1728.
- (10) Belliveau, J.; Cadwell, L.; Coleman, K.; Huwel, L.; Griffin, H. *Appl. Spectrosc.* **1985**, *39*, 727-729.
- (11) Cremers, D. A.; Radziemski, L. J. *Anal. Chem.* **1983**, *55*, 1252-1256.

- (12) Locke, R. J.; Morris, J. B.; Forch, B. E.; Miziolek, A. W. *Appl. Opt.* **1990**, *29*, 4987-4992.

Table 1

Ar sheath flow rate (slm)	S/N
1.5	90
1.0	62
0.5	102
0.3	68
0.0	50

the analyte stream relative to the laser beam. The sample was mixed with air for limit-of-detection calculations. Gas flows were controlled by mass flow meters (MKS). Separate flows of air and the diluted analyte (900 ppm) were mixed before the sample flow apparatus. The total flow rate was varied between 100 sccm and 2 slm.

OPTIMIZATION

The optimal experimental conditions for the Ar sheath of the sample probe were determined by varying the Ar flow rate. Although the primary function of the Ar sheath is isolation of the plasma from the environment, an improvement of the signal-to-noise ratio (S/N) by a factor of 2 in the presence of the sheath was observed for samples mixed with air. The S/N ratio was calculated using the intensity of the LIBS signal at the emission maximum for fluorine (685.6 nm). Table 1 lists the flow rates and the corresponding S/N for a 1% sample of CF_3H in air with a total sample flow rate of 2 slm. The optimal Ar flow rate was dependent on the sample flow rate and the position of the plasma. At Ar flow rates above 1 slm, the plasma was physically disrupted (i.e., changes in the shape, size, and position of the plasma within the boxcar-averaging time). The increase in S/N with the Ar sheath may be due to stabilization of the plasma by isolation or repositioning. The laser beam was positioned approximately $1/8$ in. above the inner tube. The instability of the plasma increased at lower vertical positions, and dilution of the analyte may occur at substantially greater vertical positions.

A plot of S/N vs laser energy (Figure 3) indicates that the optimal laser energy is approximately 120 mJ for our system (PMT/boxcar). The data were recorded with an argon sheath flow rate of 500 sccm and a 1% mixture of CF_3H /air. The signal increased 240% at 200 mJ compared to 60 mJ, but a substantial increase in the noise degraded the S/N at the higher energy. The laser amplifier was required to obtain energies above 120 mJ. An increase in the shot-to-shot variation of the laser power was observed when the laser amplifier was employed. The standard deviation of the laser energy measurements increased by factors of 1.9, 1.8, and 2.4 at 300 mJ compared to 120 mJ for three measurements of 500 laser shots. The precision of the standard deviation measurement also decreased at greater energies. The noise in the LIBS signal increased by a factor of 2.3 from 120 to 300 mJ. Also, the plasma was physically disrupted (i.e., changes occurred in the shape, position, and size of the plasma within the measurement time) at high energies (≥ 140 mJ), which could be another source of noise in the measurement.

The single-strand fiber optic studies mapped the plasma for signal intensity vs the horizontal and vertical position of the fiber optic. The acceptance angle of the fiber optic was 24° with a core diameter of 0.6 mm. The horizontal and vertical coverage of the

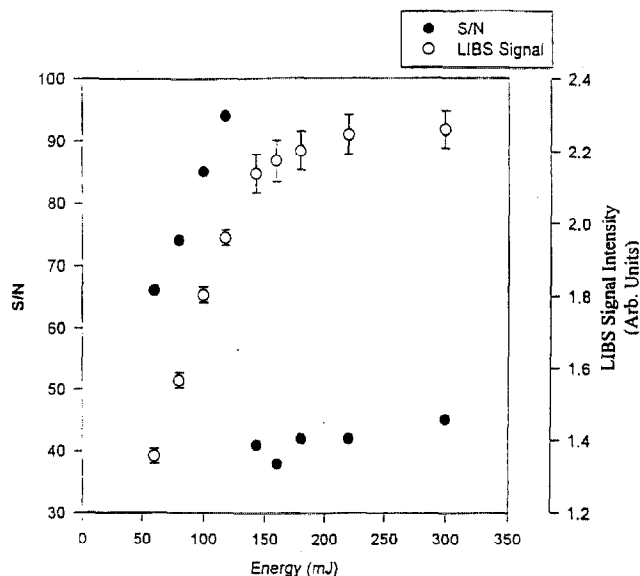


Figure 3. S/N and signal intensity of the F(I) line at 685.6 nm vs laser energy.

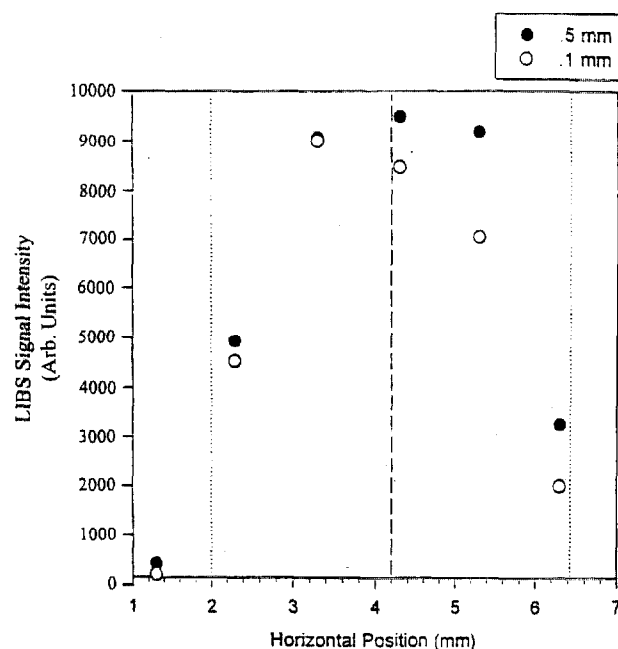


Figure 4. Signal intensity at 685.6 nm at different horizontal positions plotted for 0.5 and 0.1 mm over the bottom edge of the plasma.

fiber optic was approximately 1.3 mm. The stage was moved in increments of 1 mm. The laser beam was approximately centered over the inner tube which contained the analyte flow. A plot of LIBS signal intensity vs the horizontal position is shown in Figure 4 for two vertical positions relative to the bottom edge of the plasma. The boundaries for the visible emission from the plasma are indicated with dotted lines. The position of the limits of the plasma were estimated by locating the fiber optic/mm stage in proximity to the plasma boundaries. The signal reaches a maximum near the horizontal midsection of the plasma (dashed line). A contour plot of signal intensity at 685.6 nm for the horizontal and vertical positions of the fiber optic is shown in Figure 5. The sample was 1% CF_3H in air. The diameter of the

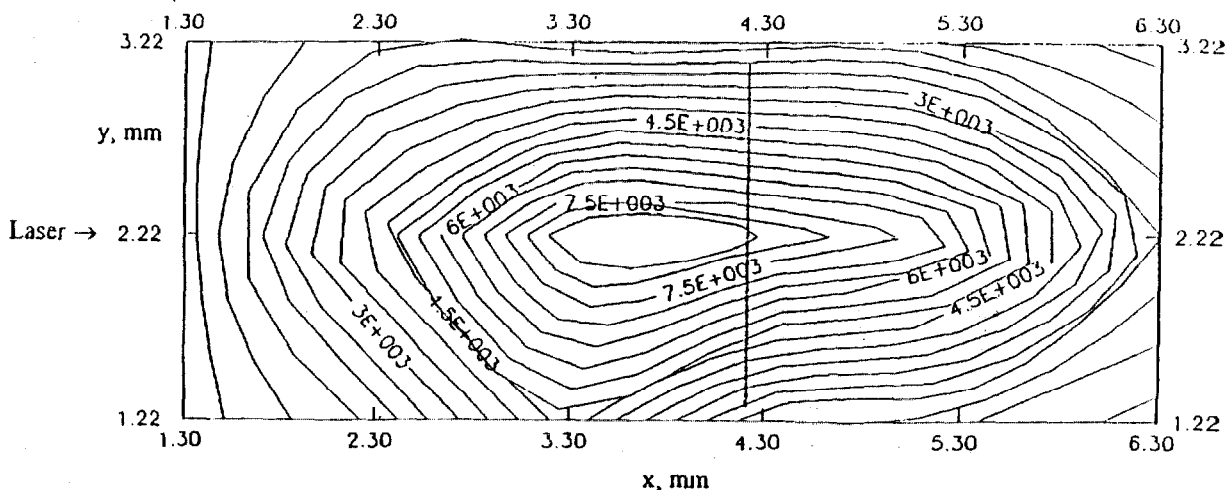


Figure 5. Contour plot for signal intensity at 685.6 nm vs different horizontal and vertical positions in the plasma.

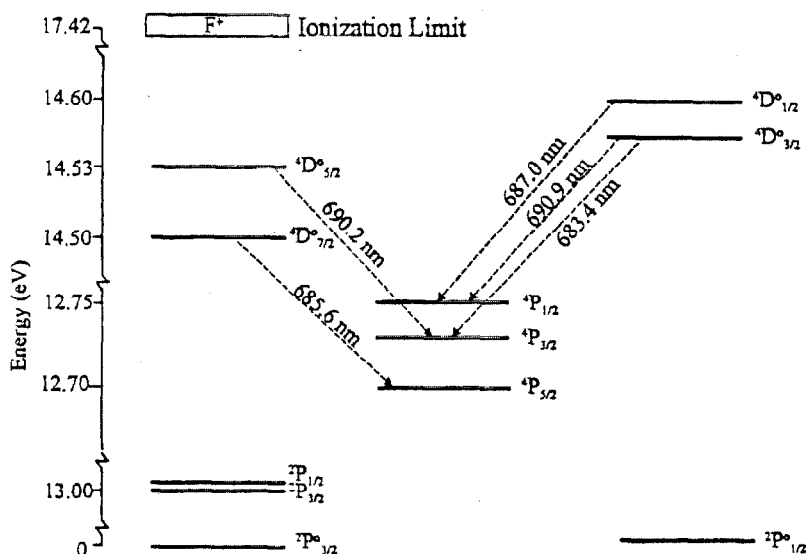


Figure 6. Partial energy-level diagram for the fluorine atom with transitions used for analysis labeled.

incident laser beam was approximately 6 mm, and the focal length of the lens was 90 mm. Thus, the diameter at the focus is approximately 0.02 mm (eq 1), where w_2 = radius at focus, f = focal length of lens, and w_1 = radius of laser beam. The beam

$$w_2 \approx (f/w_1)(\lambda/\pi) \quad (1)$$

focus should be in the vicinity of the highest contour. It is evident that a decrease in the wavelength of the laser beam will produce a more confined beam focus. Decreasing the focal length of the lens should have the same effect. The dashed line indicates the approximate horizontal center of the plasma; the vertical center was not estimated. The LIBS signal intensity maximum contour is located from the center to the direction toward the laser. The plasma also expands in this direction with an increase in laser power, which has been noted by other researchers. The region of maximum intensity is approximately 1 mm in length, and thus the position of the fiber optic for optimal response is not critical.

RESULTS AND DISCUSSION

The energy level diagram for the fluorine-atom transitions in the visible which are used for analysis is shown in Figure 6.

Neutral atoms of fluorine are detected with the LIBS technique used in this study. Atomic fluorine is generated and excited in the plasma and relaxes by fluorescence. The relative intensities of the transitions, which were determined experimentally, from 683.4–690.9 nm are 3.3, 9.4, 3.0, 6.2, and 3.0 in order of increasing wavelength for a neat plasma of CF_4 . The relative intensities were comparable for the different agents. This indicates that the plasma temperature is similar for the different agents. Typical LIBS plasma temperatures are in the 20 000–25 000 K range for gases at atmospheric pressure.⁴ Spectra of neat CF_4 collected with the PMT/boxcar system are shown in Figure 7. The boxcar-gate width was set at 1 μs . The emission due to F I is clearly resolved with the maximum intensity at 685.6 nm. Emission from F II was not observed. Emission from the Ar sheath was observed at 810.4, 811.4, 840.8, and 842.5 nm. The LIBS spectra of other agents were similar except that the intensity of the peak at 656.3 nm substantially increased due to hydrogen emission, as shown in Figure 8 for neat CF_2H_2 . This suggests a simple method to distinguish fluorocarbons and hydrofluorocarbons with LIBS and an alternative means to the fluorine lines for detecting the hydrofluorocarbons. The greater line width of the hydrogen emission relative to the fluorine lines is due to Stark broadening.

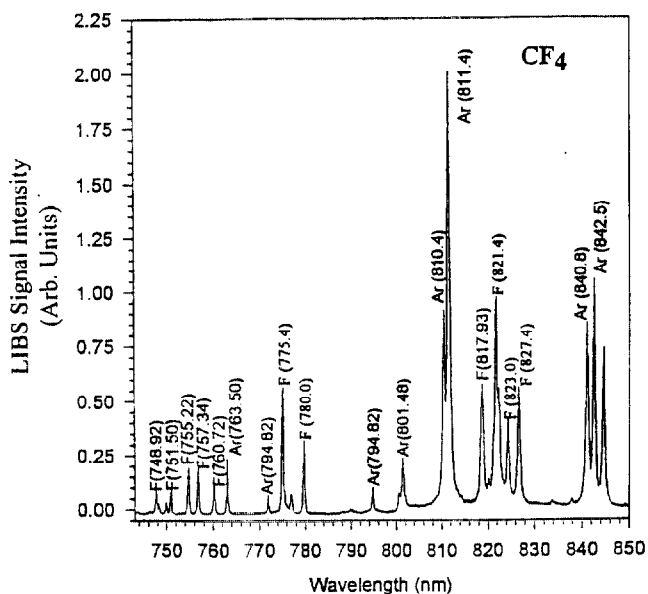
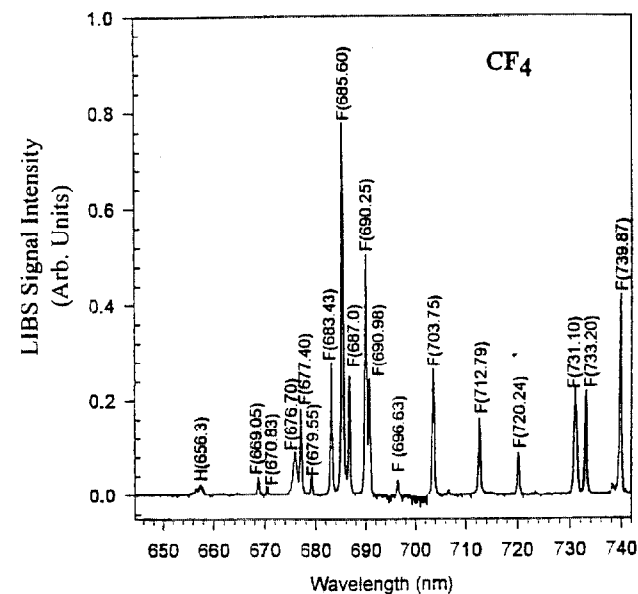


Figure 7. (A) LIBS spectrum in the visible for neat CF_4 recorded with the PMT detection system. (B) LIBS spectrum in the near-IR for neat CF_4 recorded with the PMT detection system.

The electron density which indicates the degree of ionization can be calculated using the hydrogen line width.⁴

A spectrum recorded in air (Figure 9) shows emission from nitrogen and oxygen. The main spectral region for fluorine emission is free from interferences. The peak at 685.6 nm was used to determine a limit of detection (LOD) of 40 ppm for fluorine in air using the PMT system. This LOD was calculated by multiplying the LOD obtained for CF_4 by four. This LOD was determined with a laser energy of 120 mJ. This is compared to an LOD of 38 ppm with 190 mJ of laser energy which was reported by Cremers et al.¹¹ The configuration implemented in this study does not use windows, which is an advantage for sensitivity, cost, and practicality. It was also observed by Cremers et al. that the slope of the analytical curve is proportional to the number of fluorines in the compounds.¹¹

Single-shot spectra of 1% CF_3H in air recorded with the photodiode array/fiber optic system are shown in Figure 10. The

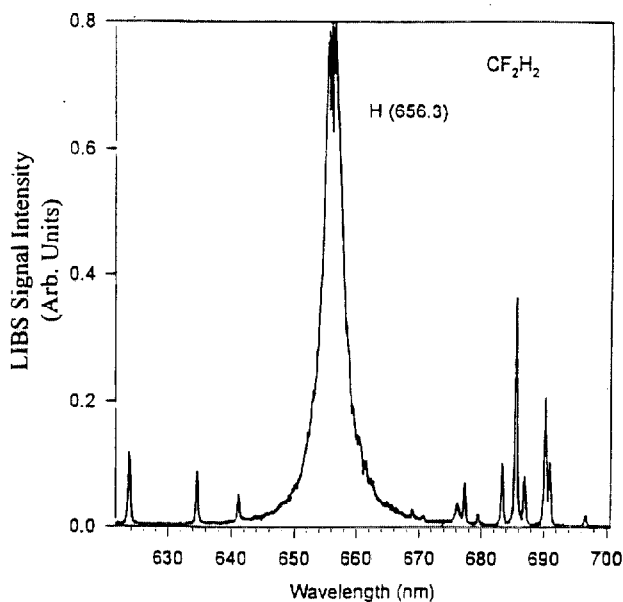


Figure 8. LIBS spectrum of neat CF_2H_2 recorded with the PMT detection system.

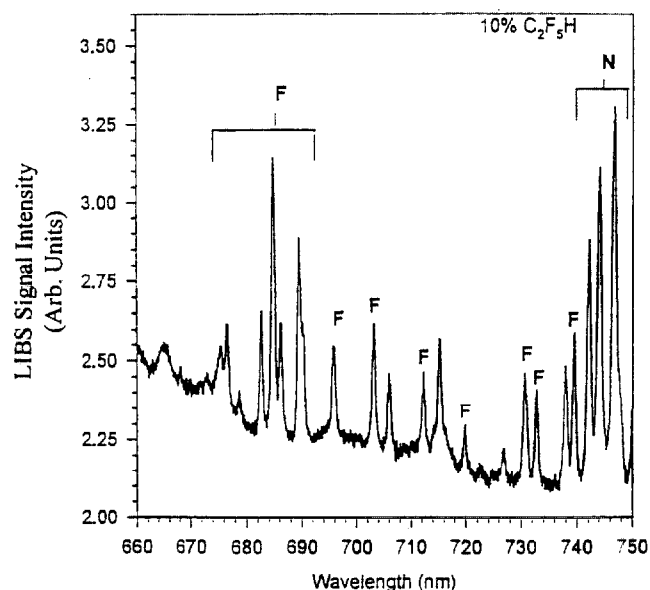


Figure 9. LIBS spectrum of 10% $\text{C}_2\text{F}_5\text{H}$ in air recorded with the PMT detection system.

photodiode array system (Figure 1) was operated in a gating mode. The pulse width of the high-voltage gating pulse was set at 20 μs . The inherent RC time constant of the photodiode array was 5 ns. The optimal delay was not experimentally determined, but 1–2 μs was routinely employed. This delay was reported in the literature for fluorine.¹¹ The noise for five consecutive measurements of shot-to-shot spectra was 8%, and the LOD for fluorine in air was 60 ppm.

The collection of one-shot spectra has significance for field measurements in fire extinguishing applications. After release of the agent, its relative distribution can be determined with nanosecond time resolution. The initial distribution of the agent and its temporal evolution are important factors in predicting the efficiency of the agent for fire suppression, safety, and determining how well the distribution system works. Multiple LIBS systems

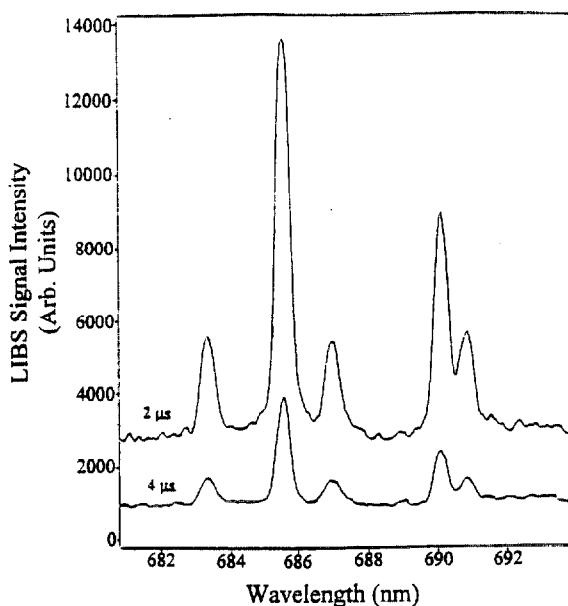


Figure 10. Single-shot LIBS spectra of 1% CF_3H in air at 2 and 4 μs delay times for the HV pulse which gates the photodiode array intensifier.

could be used to map the distribution of the agent in various locations of the test fixture. This can be accomplished inexpensively and practically with single-strand fiber optics and one charge-coupled device (CCD, two-dimensional array detector). Collection optics are not necessary for the detection fiber. Focusing optics are required to launch the excitation beam into the fiber. Applications which launch the excitation beam into a 1 mm fiber have been reported by other researchers.¹³ Advanced optical techniques make it possible to deliver > 50 mJ diffraction-

(13) Marquardt, B. J.; Goode, S. R.; Angel, S. M. *Anal. Chem.* **1996**, *68*, 977-981.

(14) Lavery, P. J. U.S. Laser Corp. Private communication.

limited and multimode beams through large core multimode fibers with almost no degradation of beam quality.¹⁴ Typical concentrations of the agents utilized in the field are 1-30%; thus, one-shot spectra can be recorded without employing objectives for the detection fiber. As mentioned earlier, positioning the emission fiber is not critical. The detector can be remote since the fibers are inexpensive and inherently low loss in the wavelength range of interest. The detection fiber can transmit to a portion of the CCD. Thus, the response of multiple LIBS detectors could be monitored simultaneously. For the fire extinguishing application, the primary information needed is an indication of the amount of agent present in a given area at a specific time.

CONCLUSIONS

LIBS is a selective and sensitive technique for the detection of halon alternatives. The field utility of LIBS for fire extinguishing applications appears feasible. Single-shot spectra can be recorded with nanosecond time precision for large-scale fire suppression tests. Detection limits are far below that required for field detection. In full-scale fire suppression tests, it is conceivable that multiple excitation/collection fibers would be used to map the distribution of an agent.

ACKNOWLEDGMENT

We acknowledge support from the ARL/NRC postdoctoral program and from the U.S. Army's Tank Automotive Command (TACOM) (Mr. Steven McCormick, project manager). We thank Dr. Robert Pastel (SCEE postdoctoral program) for helpful discussions about plasma temperatures and the laser beam focus diameter.

Received for review April 4, 1997. Accepted January 7, 1998.

AC970362Y